Fluidity of Hydration Layers Nanoconfined between Mica Surfaces

Yongsheng Leng[1] and Peter T. Cummings[1,2]

[1]*Department of Chemical Engineering, Vanderbilt University, Nashville, Tennessee 37235, USA*
[2]*Chemical Sciences Division and Center for Nanophase Materials Sciences, Oak Ridge National Laboratory, Oak Ridge, Tennessee 37831, USA*

(Received 15 July 2004; published 19 January 2005)

We perform molecular dynamics simulations to investigate the shear dynamics of hydration water nanoconfined between two mica surfaces at 1 bar pressure and 298 K. Newtonian plateaus of shear viscosity comparable to the bulk value for different hydration layers $D = 0.92$–2.44 nm are obtained. The origin of this persistent fluidity of the confined aqueous system is found to be closely associated with the *rotational dynamics* of water molecules, accompanied by fast *translational diffusion* under this confinement.

DOI: 10.1103/PhysRevLett.94.026101 PACS numbers: 68.08.–p, 61.20.–p, 81.40.Pq

The dynamics and shear properties of nanoconfined aqueous systems are of considerable interest in many areas ranging from clay swelling [1], colloidal stability [2] to biolubrication [3], and nanotribology [4]. These properties of confined water under naturally occurring conditions are also critical in many biological processes in biomolecular systems, such as water transport through ion channels and through crowded intracellular environment [5,6]. Early experimental studies [7] on surface forces between molecularly smooth mica sheets in high concentration salt solutions showed that such aqueous electrolyte solutions exhibited strong short-range repulsive hydration forces when confined within a few nanometers, which dominated the double layer repulsion and van der Waals attraction forces [Derjaguin-Landau-Verwey-Overbeek (DLVO) theory] [8]. Very recently, surface force balance (SFB) experiments on the shearing of electrolyte solutions confined between two mica surfaces demonstrate that the fluidity of the surface-attached hydration layers persists even under extreme confinement ($D < 1.0$ nm) [9]. Highly purified water (conductivity water) confined to films in the range 3.5–0 nm thickness has also been found to have a viscosity within a factor of 3 of the bulk value during the ''jump-into'' contact [10]. This contrasts markedly with the behavior of nonassociative organic films, in which according to both experiments [11] and simulations [12], viscosity increases by many orders of magnitude when confined to films thinner than about 5–8 molecular layers. This persistent fluidity of water under extreme confinement when compared to nonaqueous solvents is very surprising: in order to probe the origin of this unexpected behavior, in the present study we perform molecular dynamics (MD) simulations of water nanoconfined between moving mica sheets. Our MD results reveal that the shear viscosity of bound hydration layers is intimately related to the water dipole μ rotational correlation times. Within the range of accessible shear rates in the MD regime (10^8–10^{12} s^{-1}), we found that the shear viscosity of hydration layers with $D = 1.65$ and $D = 2.44$ nm thickness is quite close to the bulk value (~1 cP). When the thickness of the hydration layer further decreases to $D = 0.92$ nm, significant ''shear-thinning'' occurs. However, this shear-thinning behavior is limited to shear rates greater than 10^9 s^{-1}, which is very close to the inverse of the longest rotational correlation time of water dipole μ. When the shear rate is less than 10^9 s^{-1}, the shear viscosity of the hydration layer reaches a Newtonian plateau around 0.042 Pa s, about one-half of the upper-limit value estimated in SFB experiment [9]. The fast translational diffusion of water molecules is maintained under this extreme confinement.

Our molecular system consists of TIP4P [13] rigid water molecules, two mica clay surfaces, and potassium ions K^+ which balance the negative charged mica surfaces due to the substitutions of Al for Si in the tetrahedral sheets [14]. For mica, we use 2M1-muscovite mica [15], a 2:1 layered dioctahedral (hydroxy-) aluminosilicate with the muscovite formula $KAl_2(Al, Si_3)O_{10}(OH)_2$. Molecular interaction potentials (the half-layer model of mica surface [16]) include water-water, water-cation, water-mica, cation-cation, cation-mica, and mica-mica, six interactions in total, which have been proved to be successful in predicting the swelling of clays [1,16]. A bond constraint algorithm [17] for water molecules with a time step of 2 fs is implemented in MD simulation. Figure 1 shows the equilibrium molecular configuration of $D = 0.92$ nm (384 water molecules) hydration layer confined between two half-layer mica sheets. Periodic boundary conditions are applied in the lateral (x and y) directions. The simulation unit lengths in the x and y directions are 41.53 and 36.06 Å, respectively, equivalent to 32 unit cells of the mica surface. Sixty-four potassium ions K^+ are attached to the two mica surfaces to render the simulated system electrically neutral. The Ewald summation with a boundary correction term [18] is used to calculate the long-range electrostatic interactions for the 2D slab geometry. Our detailed structure calculations [19] show that adjacent to mica surface, the water oxygen density distribution for hydration layers thicker than 1 nm compares very well with the x-ray

 © 2005 The American Physical Society

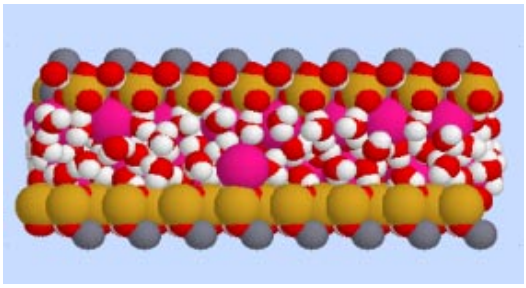

FIG. 1 (color online). The equilibrium molecular configuration of $D = 0.92$ nm (384 water molecules) hydration layer confined between two half-layer mica sheets. Atoms shown in different colors are: O (red), H (white), K (pink), Si (gold), and Al (gray).

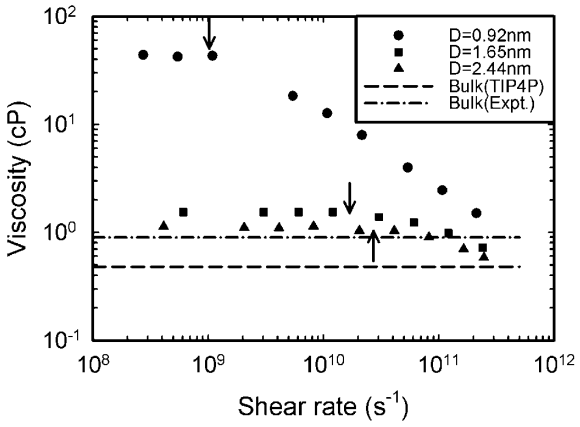

FIG. 2. The variations of shear viscosity versus shear rate for different hydration layers and the bulk water in a log-log scale. The Newtonian plateau values of the viscosity η relative to the bulk value η_0 are $\eta/\eta_0 = 2$ for $D = 2.44$ nm, 3 for $D = 1.65$ nm, and 84 for $D = 0.92$ nm. The value of the viscosity for bulk TIP4P water ($\sim$0.5 cP) is shown as a horizontal line since bulk TIP4P water is essentially Newtonian at shear rates up to at least 10^{11} s^{-1}.

reflectivity measurements, and the K^+ ions are only partially hydrated. A similar density oscillation has also been observed recently through Monte Carlo computer simulations focusing on the structure at a single surface.

To mimic the dynamics of the measurement system in SFB experiments [9,10,20], the upper mica plate is connected to a driving stage through normal and lateral springs. In order to observe the shear dynamics in MD regime, we choose the dynamic inertia of the upper mica plate equal to $2000m$ where m is the oxygen atom mass. The force constants of the normal and lateral springs are selected to be 150 and 300 N/m, respectively, the same as those in SFB experiments [20]. The contact pressure between the two mica surfaces is controlled at 1.0 bar, and the temperature of the molecular system is controlled at 298 K by applying an external bath [21] perpendicular to the shear and normal directions.

In Fig. 2, we show the variations of the shear viscosity versus shear rate for three different thickness of water layers: $D = 0.92$, $D = 1.65$, and $D = 2.44$ nm. The three molecular systems correspond to 384, 768, and 1152 water molecules confined between two mica surfaces, which are periodically replicated in the plane parallel to the surfaces. Frictional dynamics of the upper mica plate are described in the similar way as in the atomic force microscope simulations in the constant-height mode [22]. The driving velocity v of the stage varies from 0.25 m/s (corresponding to the lowest shear rate for $D = 0.92$ nm water film) to 600 m/s (corresponding to the highest shear rate for $D = 2.44$ nm water film). Upon the initiation of shearing, the velocity of the upper mica plate oscillates around the driving velocity v, and the lateral spring force oscillates with a vibration frequency slightly lower than the system resonant frequency due to the fluid damping. The shear viscosity (as measured in SFB experiment) is calculated from the mean lateral spring force that calibrates the shear force at the molecular interface. Figure 2 clearly shows that for $D = 1.65$ and $D = 2.44$ nm water films, the Newtonian plateaus (1.54 and 1.08 cP, respectively) are quite close to the value for bulk TIP4P water ($\sim$0.5 cP, obtained in nonequilibrium MD simulations [23]), which underestimates the experimental viscosity of bulk water ($=$0.894 cP [24]) by $\sim$44%. When the thickness of water film further decreases to 0.92 nm (about three water layers and also comparable to the size of the partially hydrated potassium ions, see Fig. 1), at the higher shear rates significant shear-thinning occurs, but as we see in the figure, it transits to a Newtonian regime when the shear rate is less than 10^9 s^{-1}. We will show later that this transition point corresponds to the inverse of the longest rotational correlation time of the water dipole μ. The Newtonian plateau of this ultrathin hydration layer is calculated to be 42 cP, or $\sim$80 times the bulk value. This is about one-half the upper limit (80 cP) estimated in SFB experiment [9]; however, if we consider the experimental upper limit on the viscosity relative to the experimental bulk value, this ratio is $\sim$90, somewhat above what is seen in the simulation. Here, we stress that a one order magnitude increase in shear viscosity for $D = 0.92$ nm hydration layer cannot be distinguished in the experiment due to the resolution limit of shear force response [9]. The error bars of shear viscosity at very low shear rates (the last three data) are less than 10% (i.e., less than the size of the curve symbol). At larger shear rates the error bars are even smaller (less than a few percent).

The origin of this persistent fluidity of water under extreme confinement compared to nonaqueous solvents can be probed by examining the rotational and translational dynamics of water molecules in the hydration layer. It is well known that confined liquids have a spectrum of relaxation times, whereas the transition to non-Newtonian fluids depends on the longest relaxation time [25]. Water molecules are very small polar molecules whose dynamics is dominated by their rotation and diffusion. For this rea-

son, we first studied the reorientational autocorrelation functions for different unit vectors in the water molecule reference frame and found that the longest correlation time (or equivalently the rotational relaxation time) is associated with the water dipole μ. The rotational autocorrelation functions of water dipole μ for three hydration layers, defined as the first rank Legendre polynomial in NMR experiment [23], $P_1(t) = \langle \mu(t)\mu(0)\rangle$ are plotted in Fig. 3. Clearly, $D = 0.92$ nm water film has a much longer tail than the other two thicker water films have. Decay of these autocorrelation functions from MD simulations is fitted by the Kohlrausch-Williams-Watts (KWW) stretched exponential function $\exp[-(t/\tau)^{\gamma}]$ [26]. The time integral of this function yields the corresponding correlation time τ_μ, which has an analytical form given by $[\tau/\gamma\Gamma(1/\gamma)]$ with Γ as the gamma factorial function. The fitting parameters and correlation times for the three water films are listed in Table I. These rotational correlation times are much longer than the bulk water correlation times [23,27] due to nm confinements and are also longer than the corresponding diffusion times (see below). The inverse of rotational correlation time signifies the transition shear rate beyond which fluid will behave non-Newtonian, accompanied by shear-thinning and rotational ordering [12]. These transition points are shown in Fig. 2 by arrows for the three different thickness water films. When shear rates are greater than these transition shear rates, shear-thinning becomes more obvious.

Figure 4 shows the mean-square displacement (MSD) of water molecules in the lateral (x-y) direction for different hydration layers. The in-plane diffusion or residence times of water (the time taken to diffuse ca. 3 Å) [5,29] are represented by the intercepts between the line $\langle |r_{xy}(t)|^2\rangle = 9$ Å^2 and the in-plane MSD curves, which are also listed in Table I. For comparison, the corresponding MSD curves for bulk water [28] (multiplied by a factor of 2/3) are also shown in the figure. We see that the diffusion times (or equivalently, the translational relaxation times) of water molecules in thicker water layers ($D = 1.65$ and 2.44 nm) are comparable to the bulk value, whereas the diffusion time of water in $D = 0.92$ nm film is much longer. All of the diffusion times of water in hydration layers are shorter than their corresponding rotational correlation times, suggesting that the shear-thinning is governed by the rotational dynamics. However, in SFB experiments, the shear rates ($6 \sim 1200$ s^{-1}) [9] are many orders of magnitude lower than 10^9 s^{-1}, which means that the high concentration salt solutions under extreme confinement are still Newtonian fluid. Surprisingly, if we assume that the thickness of K^+ hydration shell is $\sim$3 Å under this extreme confinement, then the mean residence time of bound water in $D = 0.92$ nm hydration layer implies that the exchange rates of water molecules are at least $\sim 10^9$ s^{-1}. This validates the hypothesis of Raviv and Klein [9] that the surface-bound hydration layers under nanoconfinement can remain very fluid and, thus, are highly efficient lubricants.

Early MD simulations [12] of n-dodecane under nanoconfinement showed that when the solvent confined to six-molecular-layer film, the rotational degrees of freedom are

TABLE I. Rotational correlation and in-plane diffusion times of water in different hydration layers and in the bulk.

D(nm)	τ(ps)	γ	τ_μ(ps)	τ_D(ps)
0.92	40.43	0.249	986.3	140.7
1.65	4.07	0.267	67.3	14.6
2.44	1.98	0.257	40.6	9.9
Bulk (TIP4P)	···	···	2.9[a]	6.8[c]
Bulk (Expt.)	···	···	0.9[b]	9.8[c]

[a]Ref. [23].
[b]Ref. [27].
[c]Ref. [28].

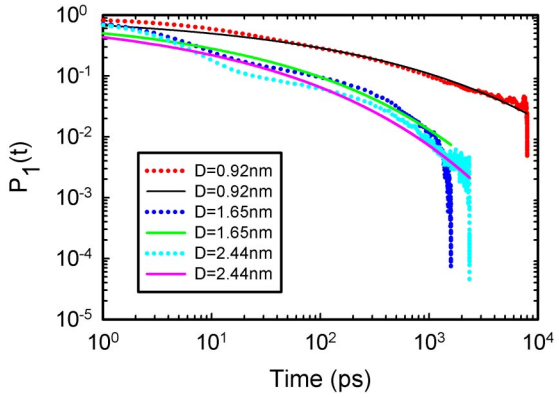

FIG. 3 (color online). Water dipole-dipole correlation functions for different hydration layers in a log-log scale. The solid lines are the fitted KWW stretched exponential functions, and the dotted lines are the calculated correlation functions from MD simulations.

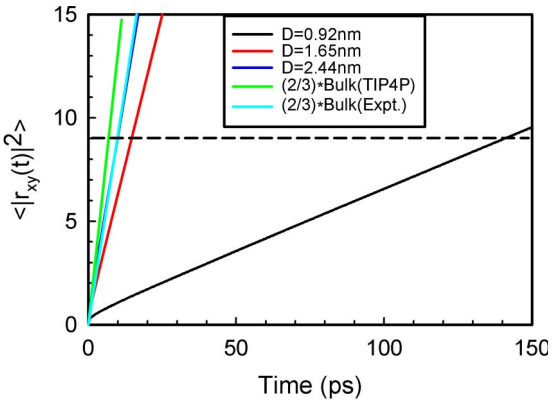

FIG. 4 (color online). Water oxygen mean-square displacements (MSD) in x-y plane as a function of time for different hydration layers and the bulk water (obtained by multiplying a factor of 2/3 of the 3D MSD of bulk water).

frozen out, and the in-plane MSD of molecular chains followed a power-law behavior. The ordered-layer structure of dodecane [12] film makes the nanoconfined material have somewhat solidlike behavior, such as the ability to sustain a finite shear stress and the stick-slip dynamics, as observed in SFB experiments [20]. Water is quite different from dodecane in that, as described above, the mobility of water molecules is still quite significant even under extreme confinement. Our MD simulations [19] also demonstrate that the partially hydrated K^+ ions are strongly bound to the negative sites of mica surfaces even though the shear rates are extremely high. Contrary to MD simulations of nonassociative organic films [12], our MD simulations do not show any ability of the bound hydration layer to sustain a finite shear stress and we do not observe any stick-slip instability—even under extreme confinement.

In conclusion, our MD simulations demonstrate the fluidity of the hydration layer under extreme confinement (from $D = 0.92$ to $D = 2.4$ nm), as observed in SFB experiments. The mechanism of this unexpected behavior has been well explained by the persistent mobility of water in the hydration layer, i.e., the fast rotational and translational dynamics of water molecules under this extreme confinement. These MD investigations of nanoconfined water at ambient condition will enhance our understanding of constraint aqueous fluids in many naturally occurring systems, such as biological and nanomechanical systems.

This work is supported by the National Science Foundation NER/CTS/PMP-0404125, Department of Energy Grant No. DE-FG02-03ER15385, and Oak Ridge National Laboratory LDRD program. The authors wish to thank Jacob Klein for helpful discussion concerning this work.

[1] E. J. M. Hensen and B. Smit, J. Phys. Chem. B **106**, 12664 (2002).
[2] R. M. Pashley and J. N. Israelachvili, J. Colloid Interface Sci. **101**, 511 (1984).
[3] D. Dowson, Proceedings of the Institution of Mechanical Engineers, Part H (Journal of Engineering in Medicine) **201**, 189 (1987).
[4] B. Bhushan, J. N. Israelachvili, and U. Landman, Nature (London) **374**, 607 (1995).
[5] B. Halle, in *Hydration Processes in Biology*, edited by M.-C. Bellissent-Funel (IOS Press, Ohmsha, 1999), p. 233.
[6] J. V. Sehy, A. A. Banks, J. J. H. Ackerman *et al.*, Biophys. J. **83**, 2856 (2002).
[7] R. M. Pashley, J. Colloid Interface Sci. **80**, 153 (1981).
[8] J. N. Israelachvili, *Intermolecular and Surface Forces* (Academic Press, London, 1985).
[9] U. Raviv and J. Klein, Science **297**, 1540 (2002).
[10] U. Raviv, P. Laurat, and J. Klein, Nature (London) **413**, 51 (2001).
[11] J. N. Israelachvili, P. M. McGuiggan, and A. M. Homola, Science **240**, 189 (1988); M. L. Gee, P. M. McGuiggan, J. N. Israelachvili *et al.*, J. Chem. Phys. **93**, 1895 (1990); H. W. Hu, G. A. Carson, and S. Granick, Phys. Rev. Lett. **66**, 2758 (1991); J. Klein and E. Kumacheva, Science **269**, 816 (1995).
[12] S. T. Cui, P. T. Cummings, and H. D. Cochran, J. Chem. Phys. **114**, 7189 (2001); S. T. Cui, C. McCabe, P. T. Cummings *et al.*, *ibid.* **118**, 8941 (2003).
[13] W. L. Jorgensen, J. Chandrasekhar, J. D. Madura *et al.*, J. Chem. Phys., **79**, 926 (1983).
[14] We assume that K^+ ions have not been exchanged by H_3O^+ ions due to the high concentration of the ions in aqueous solution [7]. This is equivalent to a high concentration monovalent salt solution used in SFB experiments [9].
[15] G. W. Brindley and G. Brown, in *Mineralogical Society Monograph No. 5* (Mineralogical Society, London, 1980).
[16] E. S. Boek, P. V. Coveney, and N. T. Skipper, J. Am. Chem. Soc. **117**, 12608 (1995).
[17] S. Miyamoto and P. A. Kollman, J. Comput. Chem. **13**, 952 (1992).
[18] I. C. Yeh and M. L. Berkowitz, J. Chem. Phys. **111**, 3155 (1999).
[19] Y. S. Leng and P. T. Cummings (to be published).
[20] J. Klein and E. Kumacheva, J. Chem. Phys. **108**, 6996 (1998); E. Kumacheva and J. Klein, *ibid.* **108**, 7010 (1998).
[21] H. J. C. Berendsen, J. P. M. Postma, W. F. Vangunsteren *et al.*, J. Chem. Phys. **81**, 3684 (1984).
[22] Y. S. Leng and S. Y. Jiang, J. Am. Chem. Soc. **124**, 11764 (2002).
[23] E. J. W. Wensink, A. C. Hoffmann, P. J. van Maaren *et al.*, J. Chem. Phys. **119**, 7308 (2003).
[24] R. C. Weast, *Handbook of Chemistry and Physics* (Chemical Rubber Corporation, Cleveland, OH, 1977).
[25] A. Berker, S. Chynoweth, U. C. Klomp *et al.*, J. Chem. Soc., Faraday Trans. **88**, 1719 (1992); S. T. Cui, P. T. Cummings, and H. D. Cochran, J. Chem. Phys. **111**, 1273 (1999).
[26] F. Muller-Plathe, J. Chem. Phys. **108**, 8252 (1998).
[27] N. Micali, S. Trusso, C. Vasi *et al.*, Phys. Rev. E **54**, 1720 (1996).
[28] M. W. Mahoney and W. L. Jorgensen, J. Chem. Phys. **114**, 363 (2001).
[29] M. Marchi, F. Sterpone, and M. Ceccarelli, J. Am. Chem. Soc. **124**, 6787 (2002).